Water Research 189 (2021) 116582

Contents lists available at ScienceDirect

Water Research

journal homepage: www.elsevier.com/locate/watres

Interaction of cyanobacteria with calcium facilitates the sedimentation of microplastics in a eutrophic reservoir

Rico Leiser[a,*], Rense Jongsma[b], Insa Bakenhus[b], Robert Möckel[c], Bodo Philipp[b], Thomas R. Neu[d], Katrin Wendt-Potthoff[a]

[a] Department of Lake Research, Helmholtz Centre for Environmental Research, Brückstraße 3a, 39114 Magdeburg, Germany
[b] Institute of Molecular Microbiology and Biotechnology, Westfälische Wilhelms-Universität Münster (WWU), Corrensstr. 3, 48149 Münster, Germany
[c] Helmholtz-Zentrum Dresden-Rossendorf, Helmholtz Institute Freiberg for Resource Technology, Chemnitzer Str. 40, 09599 Freiberg, Germany
[d] Department of River Ecology, Helmholtz Centre for Environmental Research, Brückstraße 3a, 39114 Magdeburg

ARTICLE INFO

Article history:
Received 26 June 2020
Revised 30 September 2020
Accepted 29 October 2020
Available online 30 October 2020

Keywords:
Microplastic
Reservoirs
Cyanobacteria
Calcite
Biofouling
Biofilms
Sedimentation

ABSTRACT

Low-density microplastics are frequently found in sediments of many lakes and reservoirs. The processes leading to sedimentation of initially buoyant polymers are poorly understood for inland waters. This study investigated the impact of biofilm formation and aggregation on the density of buoyant polyethylene microplastics. Biofilm formation on polyethylene films (4 × 4 × 0.15 mm) was studied in a eutrophic reservoir (Bautzen, Saxony, Germany). Additionally, aggregation dynamics of small PE microplastics (~85 µm) with cyanobacteria were investigated in laboratory experiments. During summer phototrophic sessile cyanobacteria (*Chamaesiphon* spp. and *Leptolyngbya* spp.) precipitated calcite while forming biofilms on microplastics incubated in Bautzen reservoir. Subsequently the density of the biofilms led to sinking of roughly 10% of the polyethylene particles within 29 days of incubation. In the laboratory experiments planktonic cyanobacteria (*Microcystis* spp.) formed large and dense cell aggregates under the influence of elevated Ca^{2+} concentrations. These aggregates enclosed microplastic particles and led to sinking of a small portion (~0.4 %) of polyethylene microplastics. This study showed that both sessile and planktonic phototrophic microorganisms mediate processes influenced by calcium which facilitates densification and sinking of microplastics in freshwater reservoirs. Loss of buoyancy leads to particle sedimentation and could be a prerequisite for the permanent burial of microplastics within reservoir sediments.

1. Introduction

Microplastics (MP) are frequently found in freshwater environments raising concerns about distribution pathways and ecological impacts of this novel contaminant. High loadings of MP are present in lake (Ballent et al., 2016) and reservoir sediments (Di and Wang, 2018), which may act as permanent sinks (Corcoran et al., 2015). The largest share of MP in sediments is often comprised of polyethylene (PE) which has a lower density than water (Ballent et al., 2016). Due to its physical properties this polymer type is expected to stay afloat in the water column instead of settling to the ground (Chubarenko et al., 2016).

After release into the environment, MP density, size and shape can be changed by biofouling (Kaiser et al., 2017) or aggregation with natural particles and planktonic cells (Lagarde et al., 2016). The term biofouling describes the attachment of microorganisms (biofilm formation) and macro-organisms to submerged surfaces (Rosenhahn et al., 2010). In the oceans where calcareous macro-foulers such as mussels (Kaiser et al., 2017), bryozoans (Edlin et al., 1975) or barnacles (Fazey and Ryan, 2016) are commonly found on plastics, biofouling may lead to sinking of buoyant polymers within weeks. The conditions in freshwater lakes differ from the marine environment resulting in fouling films dominated by more soft-bodied organisms (Leiser et al., 2020). Still, formation of cyanobacteria dominated biofilms can lead to the sinking of buoyant polymers (Chen et al., 2019). However, the ballasting effects of cyanobacteria (ρ: 0.990 to 1.055 g cm^{-3}) are considered being insufficient to sink buoyant MP (Li et al., 2016). Therefore it was hypothesized that the density increase originated from minerals trapped or formed inside the biofilm matrix (Chen et al., 2019).

Sessile cyanobacteria as component of aquatic biofilms play a major role in the precipitation of calcite ($CaCO_3$) (Jansson and Northen, 2010) and the subsequent lithification of biofilms (Macintyre et al., 2000) or formation of biogenic tufa (Zippel and Neu, 2011). The finding that dense biofilms ($\rho_{Biofilm} > \rho_{Water}$) may form in lakes (Chen et al., 2019) suggests that sinking of buoyant

* Corresponding author.
E-mail address: rico.leiser@ufz.de (R. Leiser).

https://doi.org/10.1016/j.watres.2020.116582
0043-1354/

MP may be facilitated by biogenic calcite precipitation. Whether the ballasting effects of freshwater biofilms are derived from the microbial biomass or from minerals was investigated in a field study.

Planktonic cyanobacteria are present in many reservoirs (Li et al., 2016) and lakes (Ortíz-Caballero et al., 2019) forming extensive blooms during late summer. *Microcystis* spp. are the most abundant phototrophs in Bautzen reservoir during July and August (Kamjunke et al., 1997). In lake water *Microcystis* spp. are aggregating to large and sinking colonies (Chen and Lürling, 2020) under the influence of dissolved Ca^{2+} (Xu et al., 2016a). These cell aggregates are often exceeding 500 µm in diameter (Feng et al., 2019), possibly enclosing small inorganic particles (Xu et al., 2016b). The question whether such *Microcystis* aggregates form under the influence of Ca^{2+} and subsequently could enclose or sink buoyant MP was studied in lab experiments.

Therefore we investigated interaction of sessile and planktonic cyanobacteria with calcium in regards of their impact on the buoyancy of PE in freshwater reservoirs.

We hypothesized that i) biofilms form on large PE in a eutrophic reservoir leading to a loss in buoyancy ii) buoyancy loss is caused by calcite precipitation iii) planktonic cyanobacteria sink small PE MP through Ca^{2+} induced aggregation. These hypotheses were tested by conducting a field experiment in the eutrophic Bautzen reservoir (Saxony, Germany) and laboratory batch experiments with calcifying cyanobacteria.

2. Material and methods

2.1. Study site

Bautzen reservoir is a freshwater body in the eastern part of Germany, providing water for cooling of coal-fired power stations, fish farming, and agricultural irrigation. It is a large (5.3 km^2) but rather shallow (mean depth 7.4 m) reservoir (Kasprzak et al., 2007), often experiencing strong winds, which sometimes even destroy the summer stratification (Kerimoglu and Rinke, 2013). Bautzen reservoir is eutrophic, with extensive blooms of *Microcystis* spp. (Kamjunke et al., 1997) occurring during summer which results in pH values up to 9.5 in the surface water. One sediment trap (Uwitec, Austria) collecting settling matter was deployed near the deepest point of the reservoir (depth: 12 m) during the year 2018 from May to December and sampled in monthly intervals.

2.2. Plastic material, exposition, and sampling procedure

Squares (4 × 4 × 0.15 mm) made from low-density polyethylene (Goodfellow ET311251, ρ: 0.924 g cm^{-3}) were incubated near the deepest point of the reservoir within a cylindrical stainless steel cage (200 particles, diameter 10 cm, length 25 cm, mesh width 3 mm) (Kettner et al., 2017). The cages had a shading effect which reduced the incoming sunlight intensity by ~33% (Leiser et al., 2020). Particles were sterilized by treatment with ethanol (70% v/v, 10 min) prior to the experiment. The cage was incubated from July 23 to August 21, 2019 (29 days) in 0.5 m depth. Profiles of oxygen concentrations, chlorophyll *a*, pH, temperature (multi-parameter probe, Sea & Sun Technologies, Germany) were measured on both dates (Figure S1).

2.3. Biofilm characterization and sampling procedures

Particles were gently removed from the cage by tweezers or by flushing with reservoir water. Particles for confocal laser scanning microscopy (CLSM) analysis were fixed in 4% v/v formalin solution right after removal from the cage. The other particles were stored in pre-combusted (450°C, 4 h) glass Petri dishes in filtered reservoir water. Additional biofilm samples were taken from the inner wall of the cage and stored in reservoir water as well. These samples were used to characterize the biofilms in regards of dry mass, mineral composition and elemental content. The PE particles were in close proximity to or even enclosed by biofilms growing on the inner cage walls. Given their visual appearance biofilms on PE were not different from biofilms from the inner cage walls (Figure S2). Therefore cage walls biofilms were considered being comparable to PE biofilms in regards of the above mentioned parameters. Most samples (except samples for DNA extraction) were stored at 8°C in the dark until processing. The densities and volumes of three fresh biofilm sub-samples from the inner walls of the cage (300 – 400 mg) and three pooled sunken PE particles were analysed with pycnometers at 25°C. Dry weight (60°C, 24 h) and ash mass (450°C, 24 h) were determined for three individual cage walls biofilm samples. The cell volume of microorganisms (biovolume) within the biofilms of ten buoyant and five sinking PE-particles was analysed via CLSM and image analysis. Particles were examined at five (floating) or ten (sinking) random locations resulting in a total sample size of 50 for each. Calcein assay (Zippel and Neu, 2011) was used to visualize Ca carbonate minerals within the biofilms of two sinking PE particles. Twenty particles for 16S amplicon sequencing were carefully rinsed with DNA-free phosphate-buffered saline (pH 7.4) and stored in liquid nitrogen. Calcium content within the cage walls biofilm dry mass was analysed by ICP-OES (detection limit: 0.1 mg l^{-1}). X-ray diffraction was used to analyse the mineral phase of cage walls biofilm dry mass.

2.4. CLSM imaging

Plastic particles with biofilms were prepared for CLSM as described elsewhere (Leiser et al., 2020). In brief: Particles were mounted and stained (SybrGreen, calcein) in Petri dishes. Imaging was done using a TCS SP5X upright microscope equipped with white laser and 63x NA 0.9 lens (Leica). Calcein staining (1 µg l^{-1}; 2 h, room temperature) was used to visualize divalent cations such as Ca^{2+} and Ca carbonate minerals (Zippel and Neu, 2011). Calcein staining is not specific for Ca^{2+} ions or calcite, and may also react with other divalent cations present in the solution. The calcein stain did not bind to pristine PE particles (data not shown). PE particles were stained with non-toxic iDye PolyPink following established protocols (Karakolis et al., 2019). Bacteria, algae and cyanobacteria were identified via SybrGreen staining, autofluorescence of chlorophyll *a* or phycobilins, respectively (Table S1 for excitation / emission wavelengths). Images were visualised and projected by Imaris (Bitplane) and presented by Photoshop (Adobe). An adaptation of ImageJ was used to semi-quantitatively calculate the biovolumes of algae, bacteria and cyanobacteria cells (Staudt et al., 2004).

2.5. Cyanobacteria cultures and laboratory aggregation experiments

The effect of dissolved Ca^{2+} on the aggregation of MP with cyanobacteria was investigated using non-axenic cultures of *Microcystis* sp. strain BM25 (Schwarzenberger et al., 2013) grown in WC media (Guillard and Lorenzen, 1972) without vitamin solution and silicate. Pre-cultures were grown on a rotary shaker (110 rpm) at room temperature and ambient daylight for 4 weeks prior to the experiment. PE powder (ρ: 0.920 g cm^{-3}; Alfa Aesar 9002-88-4) was sieved through 100 µm and 10 µm stainless steel sieves (Retsch, Germany) to obtain a defined size range of 100 – 10 µm. The mean equivalent spherical diameter (ESD) of the sieved particles was 85 ± 14 µm (n: 60). Particles were stained with iDye PolyPink (Karakolis et al., 2019). Three different Ca^{2+} concentrations (10 mg l^{-1}, 60 mg l^{-1} and, 220 mg l^{-1}) were tested for their potential to aggregate *Microcystis* sp. strain BM25.

Experiments were conducted in triplicates by inoculating 500 ml WC-media with 10 % v/v cyanobacteria pre-culture in airtight 1-liter flasks. Cell concentrations (~10^7 cells ml^{-1}) were chosen to reflect the concentration of *Microcystis* spp. in Bautzen reservoir during summer (~3 -5 × 10^7 cells ml^{-1}, data provided by the state reservoir administration of Saxony / Landestalsperrenverwaltung des Freistaates Sachsen (LTV)). Right after inoculation, samples for pH, Ca^{2+} and cell counts were taken. Directly afterwards pH was measured using a pH meter (PP-50, Sartorius). Calcium samples were filtered (0.2 µm) and stored at 4°C. Cyanobacteria cells were fixed in Lugol's iodine (5 % w/v iodine) until cell counting. Afterwards 10 mg (6.3 × 10^4 particles l^{-1}) of PE were added to the flasks. The cultures were then incubated at 23.5°C under constant light (70 W m^{-2}) on roller incubators (10 rpm) until visible aggregates formed. Depending on the Ca^{2+} concentration, aggregates formed within hours to days. Experiments showing no aggregation were stopped after 7 days. Upon termination, samples for Ca^{2+}, pH and cell counts were taken as described above. Aggregates formed within the flasks were photographed and counted employing ImageJ cell counter plugin (Rueden et al., 2017). Furthermore visible aggregates were gently removed using an inverted glass pipette. Twelve aggregates per Ca^{2+} condition (4 per triplicate) were transferred into a coverwell chamber (Thermo Fisher Scientific) for CLSM. Ca^{2+} and fluorescent MP within the sinking aggregates were visualized via CLSM. Density measurements were conducted with 9 aggregates per Ca^{2+} condition (3 per triplicate) in a temperature controlled chamber at 20°C. Aggregates were transferred to ultrapure water (20°C) and titrated with NaI (2 g ml^{-1}, ρ: 1.690 g cm^{-3}) until neutral buoyancy was achieved. The density of the resulting solution was measured with pycnometers. Sinking velocities of 30 individual aggregates (10 per triplicate) were determined in a column (diameter 5 cm) filled with tap water (20°C) and recorded with a camera (13 megapixel, 30 fps). Afterwards the same aggregates were removed from the column and checked for their plastic content under a light microscope. The ESDs of sinking aggregates were calculated from the recorded images using ImageJ. Sunken biomass/aggregates remaining after aggregate selection and sampling were filtered onto a stainless steel sieve (47 mm, pore size 10 µm) to remove non-aggregated cells. The filters were subsequently rinsed three times with ultrapure water. The biomass was dried (60°C, 24 h) and analysed for its mineral content using XRD. Cell concentrations were determined by epifluorescence microscopy after SybrGreen staining. Calcium concentrations in the media were measured via ICP-OES.

2.6. X-ray diffraction

X-ray diffraction was performed using a PANalytical Empyrean diffractometer, equipped with a Co-tube, automatic divergence slit and PIXcel 3D detector. Field samples were sieved (< 4 mm) to remove PE squares and filled into 27 mm sample holders. Measurements were performed from 5 to 80 °2θ with a stepsize of 0.0131 °2θ and total measurement time of 2 h 30 min. The irradiated area on the sample was kept constant at 12 × 15 mm by means of respective mask and the automatic divergence slit. Samples from laboratory experiments showing low mass on stainless steel filters were prepared on silicon low background holders and measured under the same conditions. Data were evaluated by the use of PANalytical's HighScore software and the BGMN/Profex package v4.0.2 (Doebelin and Kleeberg, 2015).

2.7. DNA extraction, Illumina sequencing and bioinformatics

Total DNA was extracted using the DNA Power Soil Pro Kit (Qiagen) with modifications. Biofilm covered plastic particles were transferred into the PowerBead Pro Tubes containing 800 µl of solution CD1. The tubes were fixed horizontally to a vortex adapter and shaken for one hour for mechanical disruption of bacteria. Afterwards samples were incubated for one hour with 25 μl proteinase K (22 mg ml^{-1}) at 37°C. The extraction was continued following the instructions given by the supplier. Libraries, sequencing and data analysis were performed by Microsynth AG (Balgach, Switzerland). To assess the bacterial diversity, the V4-V5 region of the bacterial 16S rRNA gene was amplified by two-step PCR using the primer pair 515F-Y and 926R (Parada et al., 2016). Libraries were sequenced using a v2 500 cycle kit and the Illumina MiSeq platform. The raw data were submitted to the ENA (European Nucleotide Archive) database and were assigned the BioProject ID: PRJEB38919. Standard statistical analysis and bioinformatics were employed to obtain relative abundance of the bacterial phyla (S3). The OTUs assigned to *Cyanobacteria* were further classified using BLAST analysis (Altschul et al., 1990) using nucleotide database (nt/nr) with uncultured and environmental sample sequences excluded.

2.8. Statistical analysis and programs

Visual MINTEQ (Version 3.1, Royal Swedish Academy of Science) was employed to calculate the saturation indices of calcite ($SI_{calcite}$) in Bautzen reservoir for the years 2018 and 2019 using the default thermodynamic database. The dataset used for modelling contained major water anions, cations, pH, temperature and chlorophyll content of Bautzen reservoir and has been provided by the LTV. Data normality was checked via Q-Q Plots and histograms. F-test was used to test for variance homogeneity prior to conducting t-tests and ANOVA. Differences between datasets were seen as statistically significant for $p < 0.05$. Akaike information criterion method was used to select the best fitting multiple linear models. Residual plots were examined for the validity of the linear models. Non-parametric rank-based tests and median statistics were used for non-normally distributed data. R (R Core Team, 2018) was used for statistical analysis and for the graphs.

3. Results & discussion

3.1. Calcite precipitation in Bautzen reservoir

Summer blooms of phototrophic microorganisms accompanied by high pH values and the decline of dissolved Ca^{2+} in surface water (Figure S3) were observed in 2018 and 2019. Calcium made up between 0.9% and 6.3% of the settling matter during June-July and July-August 2018 (Table S2). Assuming that this Ca was present solely in the form of calcite this mineral accounted for 0.24 – 2.23 g m^{-2} d^{-1} or up to 16.7% of the total settling matter during this time. Bautzen reservoir has a lower potential for calcite precipitation in the surface water compared to lakes such as Baldeggersee (Luzern, Switzerland) producing 10 – 20 g calcite m^{-2} day^{-1} (Teranes et al., 1999) or Lake Constance (Switzerland, Germany, Austria) with 14 g m^{-2} d^{-1} (Stabel, 1988). Calcite precipitation is of high importance for matter flux in many eutrophic and mesotrophic lakes, whereas being less intense in hyper-eutrophic and oligotrophic water bodies (Koschel et al., 1983).

3.2. Field biofilms and microplastic biofouling in Bautzen reservoir

The incubation cage and PE-particles were covered by dense brownish biofilms after the incubation period of 29 days. Whitish minerals (Fig. 1a) covered the biofilms surfaces and calcein stainable minerals were found in close proximity to cyanobacterial cells (Fig. 1b).

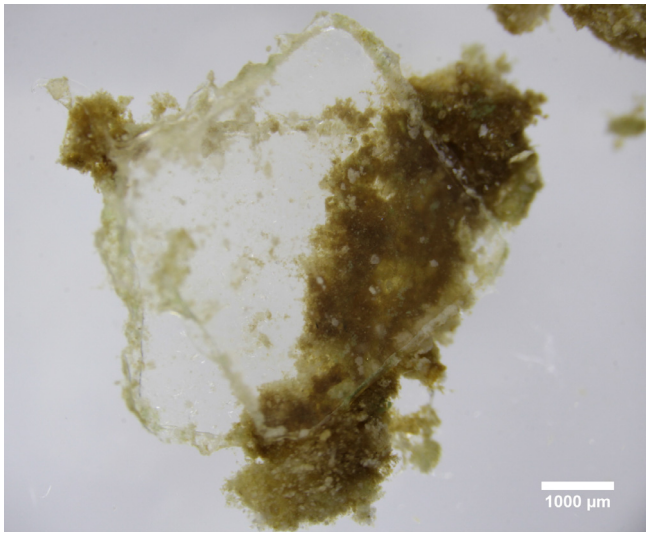

(a)

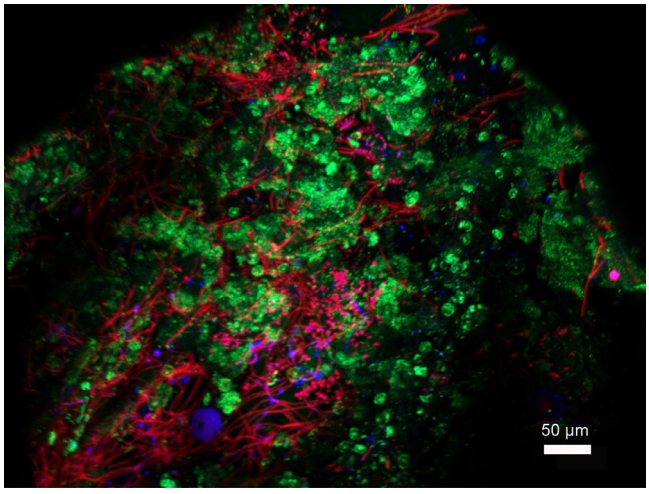

(b)

Fig. 1. Binocular image (white bright field, 10x magnification) (a) showing the biofilm covered PE particles and white mineral precipitation within the covering biofilms. CLSM image (b) showing cyanobacteria, (red, purple) and calcite (green) within the biofilms on PE particles. (For interpretation of the references to color in this figure legend, the reader is referred to the web version of this article.).

This mineralized appearance of the biofilm was reflected by the high dry mass (19.5 ± 3.6%, n: 3) and ash content (91.2 ± 1.9%, n: 3). Mineral phases of the cage walls biofilms were comprised of 98% pure calcite and 2% quartz as shown by XRD analysis (Figure S4). The contents of major elements within the cage walls biofilms dry mass were 0.2% Al, 31.1% Ca, 0.3% Fe, 0.4% Mg, 0.1% Mn, and 0.12% Si. As Ca appeared solely in the form of calcite ($CaCO_3$) this mineral accounted for ~78% of the biofilms dry mass. The calcite content of Bautzen reservoir biofilms was higher compared to biofilms found in Lake Velence (30% calcite) (Záray et al., 2005) and the Sanjiadian reservoir (20 – 40%) (Tianzhi et al., 2014). Thus calcite seems to be a common and major component of biofilms in lakes of different trophic states and water chemistry. The respective wet density of the calcified biofilms was 1.18 g cm^{-3} ± 0.012 (n: 3, 20°C). Given the similarity of cage walls biofilms and PE biofilms (Figure S2) results might be extrapolated to the MP particles. However, it cannot be excluded that biofilm properties slightly differed, which should be considered while interpreting the results.

The community composition within the biofilms of buoyant and sunken PE particles was examined via CLSM and 16S amplicon sequencing. CLSM analysis showed that the sunken particles had significantly higher cell volumes of bacteria (0.43 to 0.007 μm^3 μm^{-2}), cyanobacteria (0.09 to 0.0002 μm^3 μm^{-2}) and algae (0.03 to 0 μm^3 μm^{-2}) if compared with the buoyant particles (Fig. 2). Cyanobacteria occurred either as filamentous colonies of elongated thin cells which were found in 85% of the analysed images (n: 50) or as colonies of rounded cells found in 28% of the images (n: 50). Classification of the 16S rRNA gene sequences revealed a dominance of non-phototrophic bacteria (66% of all sequences, Fig. 3). Still a significant abundance (34%) of cyanobacteria was detected within the calcifying biofilms. Only 12 different bacterial phyla were found on the particles. Such low OTU richness has been described previously as a common feature of microbial biofilms on MP (Amaral-Zettler et al., 2020). The non-phototrophic phyla found in this study have already been described by other authors to colonize MP exposed to river or lake water (Hoellein et al., 2014; Wang et al., 2020; Wu et al., 2019).

Within the cyanobacteria GpI were the most abundant group (26%), followed by GpV (7%), and GpIIa (1%) (Fig. 3). Based on further classification of the sequences using BLAST analysis (Altschul et al., 1990) the groups GpI and GpV could be assigned to *Chamaesiphon* spp. and *Leptolyngbya* spp. According to their morphology, the colonies of rounded cells could belong to *Chamaesiphon* spp. (Kurmayer et al., 2018) whereas the filamentous colonies, which were found in most of the images, resembled *Leptolyngbya* spp. (Arp et al., 2010) cells. Both genera, *Chamaesiphon* spp. (Peraza Zurita et al., 2005) and *Leptolyngbya* spp. (Zippel and Neu, 2011), are common members of calcifying freshwater biofilms (Arp et al., 2010). Especially *Leptolyngbya* spp. has been associated with an increase of $SI_{Calcite}$ and calcite precipitations within stream biofilms (Brinkmann et al., 2015). Further, calcite grains are often found in close proximity or even encrusting cyanobacterial cells (Martinez et al., 2010), which was also observed in our study using calcein staining (Fig. 1b). Hence it is likely that calcite was precipitated by cyanobacteria leading to densification of the biofilms and subsequent sinking of the PE particles. Still heterotrophic bacteria might have influenced the calcite precipitation by providing nucleation sites or releasing Ca^{2+} bound to the organic biofilm matrix (López-García et al., 2005). As algae and diatoms were scarce throughout, occurring in only 10% of the image datasets (n: 50), their influence on calcite precipitation might have been minor.

PE particle buoyancy was tested by observing their upward or downward movement in water. Approximately 20 to 30 particles (10 – 15%) lost their buoyancy at the end of the field experiment. For a minor fraction of PE particles physical disturbance by the sampling procedure led to a certain loss of biofilm and consequently to regaining of their buoyancy. The interior of the cage was covered with biofilms entrapping and hiding some of the PE particles. As a consequence the proportion of sunken particles could not be estimated precisely leading to the conservative number of 20 to 30 sunken particles. The density of the sunken PE-particles was 1.19 g cm^{-3} at 20°C (n: 1), which implies a sharp density increase compared to pristine particles (ρ: 0.924 g cm^{-3}). Biofilm formation has already been reported to sink buoyant MP within 18 days in shallow and high productive lakes (Chen et al., 2019). The authors hypothesized that minerals (calcite, clays) trapped within the biofilms rather than the microbial cells induced sinking of the MP (Chen et al., 2019). In the present study a biofilm volume of 2.68 × 10^{-2} cm^3 (n: 1) was bound to the sunken MP from Bautzen reservoir of which only ~ 1.85 × 10^{-6} cm^3 (n: 50) was accounted for by cells. The main part of the fouling film (collected from cage walls) was comprised of water (around 77% of the weight), organic material (around 2%) and inorganic components (around 21%) with

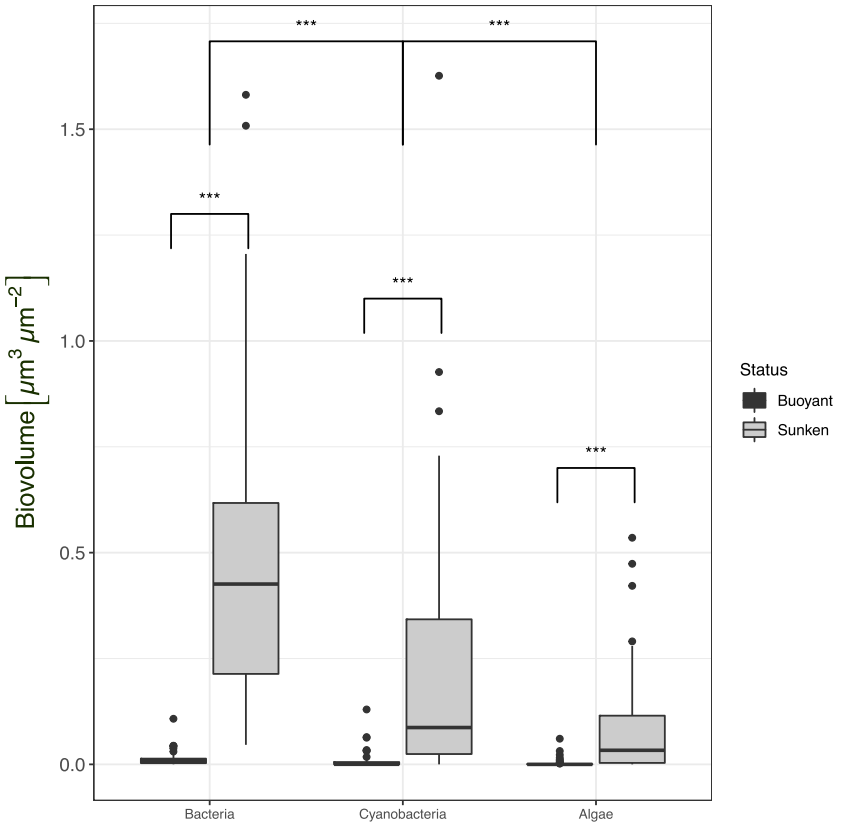

Fig. 2. Biovolumes of bacteria, cyanobacteria and algae cells in biofilms on PE particles retrieved from Bautzen reservoir after 29 days of incubation. Biovolumes were semiquantitatively measured via CLSM followed by image analysis. Significant differences are displayed by asterisks ***: $p < 0.001$.

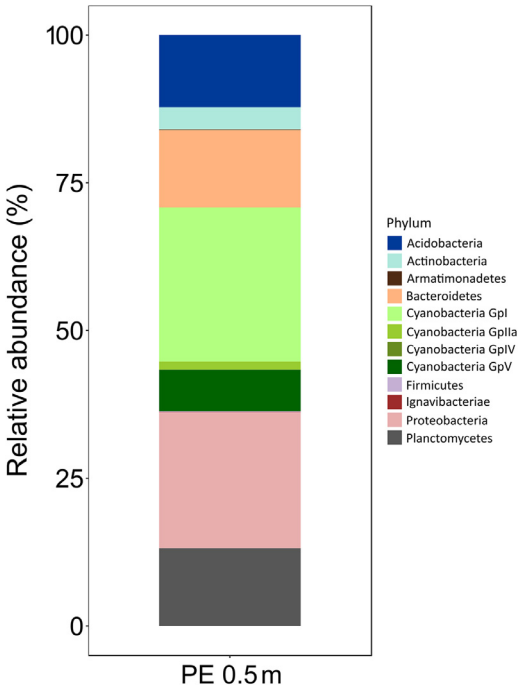

Fig. 3. Bacterial community composition (phylum level) on PE particles exposed in Bautzen reservoir as obtained via 16S sequencing. GpI: Chamaesiphon spp.; GpV: Leptolyngbya spp.; GpIIa: Synechococcus spp.

calcite constituting 17% of the total biofilm weight. Therefore it can be assumed that the contribution of organic matter and microbial cells to the overall biofilm density was minor compared to biogenic calcite.

In marine environments similar studies found that buoyant MP will sink within 2 to 6 weeks (Fazey and Ryan, 2016; Kaiser et al., 2017) due to the development of fouling films on their surfaces. Results of different studies are not easily transferable since the effect of biofouling on MP density is related to particle surface to volume ratio, which is influenced by particle specific size and shape (Chubarenko et al., 2016). MP films are more susceptible towards biofouling than fibers or spheres (Chubarenko et al., 2016), while small particles will lose buoyancy faster than large particles (Fazey and Ryan, 2016). However, the effect of biofouling has only been described for large particles yet. Given by their small size, sub-millimeter MP particles will be colonized by different organisms compared to large plastics (Rogers et al., 2020). Therefore it remains uncertain if findings made for larger plastics can be transferred to small MP (< 1 mm). Hence our finding that calcite formation reduces the buoyancy of large PE films might not be extrapolated to particles smaller than 1 mm. Furthermore it should be considered that the used PE films represented only a small part of the different shapes and size classes of MP found in freshwater. As size and shape influence the surface to volume ratio, these parameters have to be carefully taken into account when transferring the results of this study to other types of particles.

3.3. Calcium, cyanobacteria and MP aggregation in lab experiments

Sinking aggregates of *Microcystis* spp. cells formed under the influence of 220 mg l^{-1} and 60 mg l^{-1} Ca^{2+} after < 2 h and 2 days, respectively, while no aggregates formed under 10 mg l^{-1} Ca^{2+} within 7 days. Each of the experimental approaches reached pH ~ 9.7 at the end of the experiment. Declining of Ca^{2+} concentration was not detected during the experiments. Calcite or other mineral

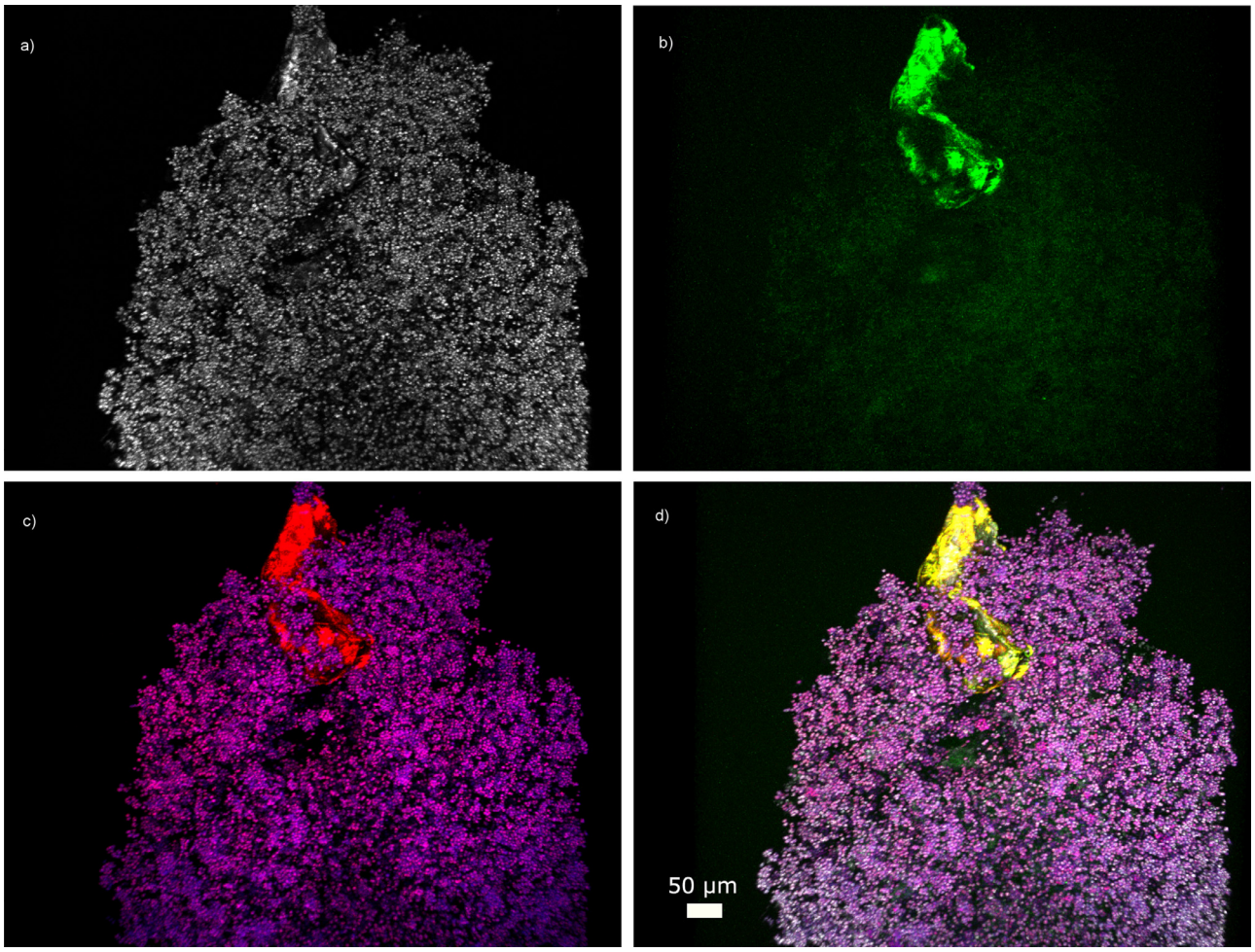

Fig. 4. CLSM images of an aggregate formed during precipitation experiments (60 mg l^{-1} Ca^{2+}), different laser channels are displayed showing a) total reflection (white), b) calcein (green), c) cyanobacteria (purple) and PE (red) and d) the resulting composite image. (For interpretation of the references to color in this figure legend, the reader is referred to the web version of this article.).

phases were not found within the aggregates employing XRD analysis.

PE particles were incorporated into the matrix (Figure S5) or attached to the outer side of the aggregates. Some of the polymer particles were encrusted by calcein stainable matter (Fig. 4). The aggregates formed in 60 mg l^{-1} and 220 mg l^{-1} Ca^{2+} incorporated on average 2 MP particles (mean, n: 60) and subsequently transported them to the bottom of the incubation flasks (Fig. 5). Each flask contained approximately 65 aggregates (mean, n: 5) which in sum incorporated ~130 PE particles (~0.4% of added particles).

Aggregation and settling of MP with eukaryotic algae (Lagarde et al., 2016) and diatoms (Long et al., 2015) have been reported before. So freshwater algae *Chlamydomonas reinhardtii* formed dense aggregates (ρ: 1.2 g cm^{-3}) with polypropylene MP readily sinking in culture media (Lagarde et al., 2016). The aggregates in our study were denser than water (ρ: 1.1 g cm^{-3} for 60 mg l^{-1} Ca^{2+}; 1.05 g cm^{-3} for 220 mg l^{-1} Ca^{2+}) (Fig. 5) and slightly exceeded the density ranges previously reported for cyanobacterial aggregates (1.01 -1.05 g cm^{-3}) (Li et al., 2016). Aggregate densities might be influenced by strain specific excretion of extracellular polymeric substances (EPS) (Li et al., 2016) or formation of gas vacuoles (Xu et al., 2016a). Furthermore, the density of such aggregates strongly depends on other external factors such as the seasons (Li et al., 2016). Under favourable environmental conditions such as high temperature, nutrient loadings or light intensities (Li et al., 2016) cyanobacterial aggregates may stay afloat instead of sinking to the sediments. Multiple linear regression modelling revealed that sinking speed of the aggregates was dependent solely on their size, with larger colonies settling faster than smaller ones. Aggregates in 60 mg l^{-1} Ca^{2+} were significantly larger (mean: 1519 µm, n: 30) than the aggregates formed in 220 mg l^{-1} Ca^{2+} (mean 1262 µm, n: 30). Therefore they were settling approximately 25 % faster than the smaller aggregates (Fig. 5). Regarding the longer incubation time (2 days for 60 mg l^{-1} Ca^{2+} and 1 day for 220 mg l^{-1} Ca^{2+}) this might have been a temporal effect rather than depending on the Ca^{2+} concentration. Considering the sinking velocity of the aggregates (0.0036 m s^{-1} for 60 mg l^{-1} Ca^{2+} and 0.0029 m s^{-1} for 220 mg l^{-1} Ca^{2+}), aggregation with cyanobacteria may transport buoyant small PE to the sediment of Bautzen reservoir within 34 to 42 minutes. However, this might only hold true for MP particles being smaller than the enclosing cyanobacterial aggregates. Large particles (1- 5 mm), such as the PE films used in the field study, are unlikely to be incorporated into the cyanobacterial aggregates (~1 - 1.5 mm). Therefore the results might only be applicable for MP smaller than 100 µm.

Most likely aggregation of cyanobacterial cells was induced by the elevated Ca^{2+} concentrations used in our study. Ca^{2+} ions are suspected to form bridges between the negatively charged cyanobacteria or EPS (Xu et al., 2016a), leading to the formation of cell aggregates (Chen and Lürling, 2020). Furthermore elevated Ca^{2+} concentrations can increase the production of cyanobacteria

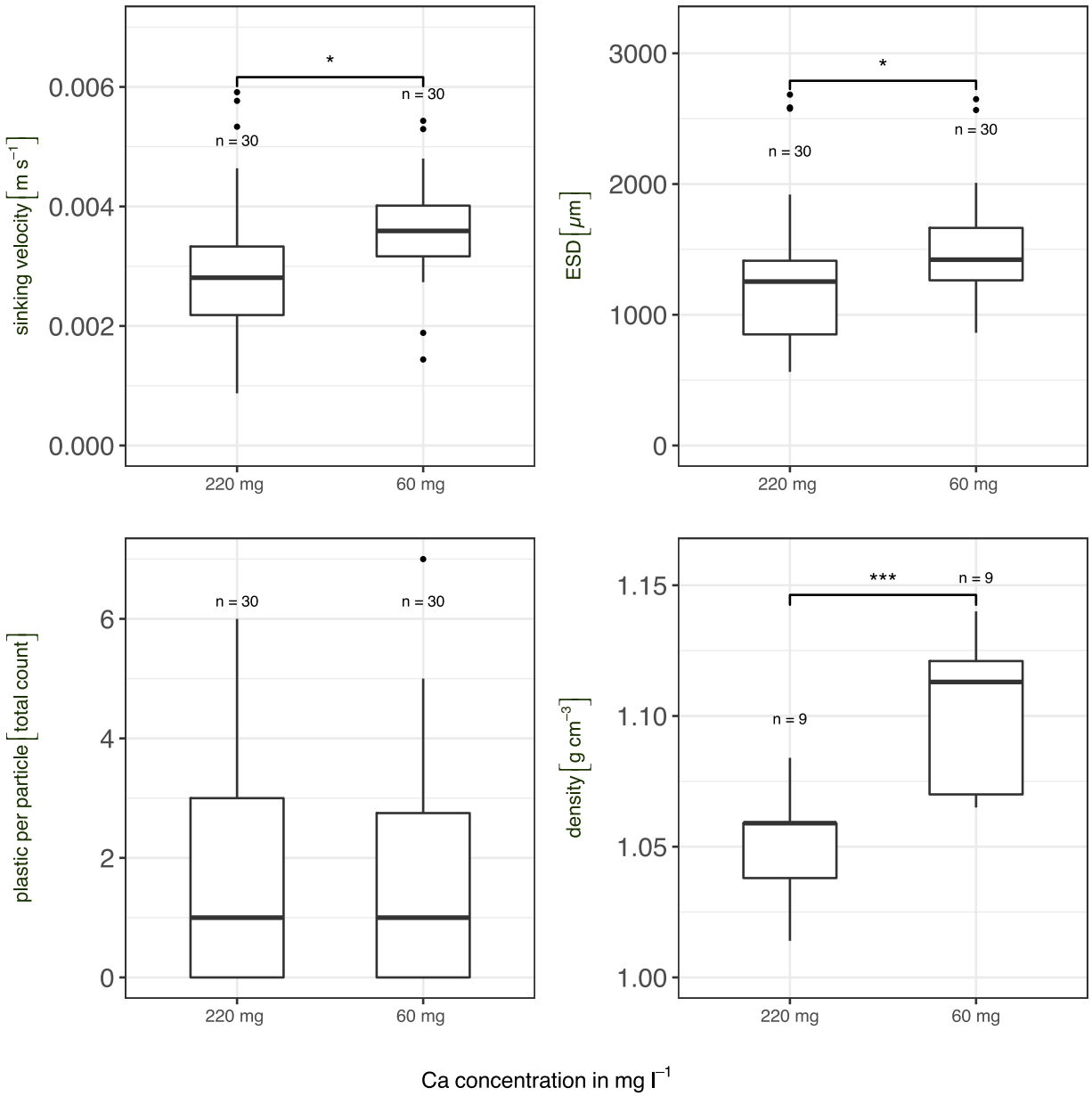

Fig. 5. Properties of cyanobacterial aggregates formed under high (220 mg l^{-1}) and intermediate (60 mg l^{-1}) Ca^{2+} concentrations. Significant differences are displayed as asterisks ***: $p < 0.001$ and *: $p < 0.05$.

EPS (Wang et al., 2011), which plays a crucial role in aggregation processes by providing a sticky, flexible and robust matrix in which cells are embedded (De Oliveira et al., 2020). The assumed bridging role of Ca^{2+} can be supported by the presence of calcein stainable matter within the aggregates (Fig. 4) connecting the cyanobacterial cells. Ca^{2+} concentrations >20 mg l^{-1} are required to induce aggregation of cyanobacterial cells (Chen and Lürling, 2020). Bautzen reservoir has a median Ca^{2+} concentration of 35 mg l^{-1}, which lies in the usual range (10 -120 mg l^{-1} Ca^{2+}) of freshwater bodies (Wang et al., 2011). Correspondingly, large cyanobacterial aggregates / colonies were observed in Bautzen reservoir during the samplings in 2018 and 2019 (Figure S6). This leads to the assumption that the aggregation of cyanobacteria through Ca bridging might be relevant for the fate of small MP in Bautzen reservoir. The Ca^{2+} concentrations used in the lab experiments did not reflect the actual concentrations found in Bautzen reservoir. Still we could show that *Microcystis* spp. aggregate with MP under environmentally relevant Ca^{2+} concentrations (60 mg l^{-1}).

Field and lab experiments described two distinct processes leading to sinking of buoyant PE microplastics in the context of cyanobacterial interaction with calcium. Apparently the formation of biofilms sank proportionally more particles (~ 10 -15%) than the aggregation of small PE with cyanobacteria. However, the low removal efficiency rather resulted from the low concentration of cyanobacterial aggregates (mean: 130 aggregates l^{-1}) than from the number of PE particles incorporated into each of the aggregates (mean: 2). Taking into account that, during cyanobacteria blooms concentrations of 3.5×10^5 aggregates l^{-1} can be reached (Feng et al., 2019), aggregation governs a high potential for MP removal in productive lakes.

4. Conclusions

- A proportion of polyethylene microplastics (~10 - 15% of particles) lost its buoyancy due to biofilm formation after being exposed for 29 days in a eutrophic reservoir

- Biofilms were rich in calcite. Apparently the mineral had a greater effect on biofilm density compared to organic matter or cells
- Cyanobacteria *Chamaesiphon* spp. and *Leptolyngbya* spp. were abundant biofilm members probably facilitating calcite formation in the biofilms
- Planktonic cyanobacteria formed sinking aggregates with small polyethylene microplastics (enclosing ~0.4% of particles) under elevated Ca concentrations

Funding sources

This research was supported by the BMBF project MikroPlaTaS (02WPL1448A). The authors declare no competing financial interest.

Declaration of Competing Interest

The authors declare that they have no known competing financial interests or personal relationships that could have appeared to influence the work reported in this paper.

Acknowledgment

We thank Ute Kuhlicke for her eminent help with confocal microscopy and Corinna Völkner for her expertise in conducting field work. The Landestalsperrenverwaltung des Freistaates Sachsen and Alice Rau are acknowledged for their kind help in providing water data and access to Bautzen reservoir. Furthermore we thank Anke Schwarzenberger for providing *Microcystis* sp. strain BM25 for the lab experiments.

Supplementary materials

Supplementary material associated with this article can be found, in the online version, at doi:10.1016/j.watres.2020.116582.

References

Altschul, S.F., Gish, W., Miller, W., Myers, E.W., Lipman, D.J., 1990. Basic local alignment search tool. J. Mol. Biol. 215, 403–410. doi:10.1016/S0022-2836(05)80360-2.

Amaral-Zettler, L.A., Zettler, E.R., Mincer, T.J., 2020. Ecology of the plastisphere. Nat. Rev. Microbiol. 18, 139–151. doi:10.1038/s41579-019-0308-0.

Arp, G., Bissett, A., Brinkmann, N., Cousin, S., de Beer, D., Friedl, T., Mohr, K.I., Neu, T.R., Reimer, A., Shiraishi, F., Stackebrandt, E., Zippel, B., 2010. Tufa-forming biofilms of German karstwater streams: microorganisms, exopolymers, hydrochemistry and calcification. Geol. Soc. Spec. Publ. 336, 83–118. doi:10.1144/SP336.6.

Ballent, A., Corcoran, P.L., Madden, O., Helm, P.A., Longstaffe, F.J., 2016. Sources and sinks of microplastics in Canadian Lake Ontario nearshore, tributary and beach sediments. Mar. Pollut. Bull. 110, 383–395. doi:10.1016/j.marpolbul.2016.06.037.

Brinkmann, N., Hodač, L., Mohr, K.I., Hodačová, A., Jahn, R., Ramm, J., Hallmann, C., Arp, G., Friedl, T., 2015. Cyanobacteria and diatoms in biofilms of two karstic streams in Germany and changes of their communities along calcite saturation gradients. Geomicrobiol. J. 32, 255–274. doi:10.1080/01490451.2014.901438.

Chen, H., Lürling, M., 2020. Calcium promotes formation of large colonies of the cyanobacterium *Microcystis* by enhancing cell-adhesion. Harmful Algae 92, 101768. doi:10.1016/j.hal.2020.101768.

Chen, X., Xiong, X., Jiang, X., Shi, H., Wu, C., 2019. Sinking of floating plastic debris caused by biofilm development in a freshwater lake. Chemosphere 222, 856–864. doi:10.1016/j.chemosphere.2019.02.015.

Chubarenko, I., Bagaev, A., Zobkov, M., Esiukova, E., 2016. On some physical and dynamical properties of microplastic particles in marine environment. Mar. Pollut. Bull. 108, 105–112. doi:10.1016/j.marpolbul.2016.04.048.

Corcoran, P.L., Norris, T., Ceccanese, T., Walzak, M.J., Helm, P.A., Marvin, C.H., 2015. Hidden plastics of Lake Ontario, Canada and their potential preservation in the sediment record. Environ. Pollut. 204, 17–25. doi:10.1016/j.envpol.2015.04.009.

De Oliveira, T.T.S., Andreu, I., Machado, M.C., Vimbela, G., Tripathi, A., Bose, A., 2020. Interaction of cyanobacteria with nanometer and micron sized polystyrene particles in marine and fresh water. Langmuir 36, 3963–3969. doi:10.1021/acs.langmuir.9b03644.

Di, M., Wang, J., 2018. Microplastics in surface waters and sediments of the Three Gorges Reservoir. China. Sci. Total Environ. 616–617, 1620–1627. doi:10.1016/j.scitotenv.2017.10.150.

Doebelin, N., Kleeberg, R., 2015. Profex: a graphical user interface for the Rietveld refinement program BGMN. J. Appl. Crystallogr. 48, 1573–1580. doi:10.1107/S1600576715014685.

Edlin, G., Lin, L., Kudrna, R., 1975. Plastic films on the bottom of the Skagerack. Nature 255, 735–737. doi:10.1038/253600a0.

Fazey, F.M.C., Ryan, P.G., 2016. Biofouling on buoyant marine plastics: an experimental study into the effect of size on surface longevity. Environ. Pollut. 210, 354–360. doi:10.1016/j.envpol.2016.01.026.

Feng, B., Wang, C., Wu, X., Tian, C., Zhang, M., Tian, Y., Xiao, B., 2019. Spatiotemporal dynamics of cell abundance, colony size and intracellular toxin concentrations of pelagic and benthic *Microcystis* in Lake Caohai, China.. J. Environ. Sci. 84, 184–196. doi:10.1016/j.jes.2019.05.010.

Guillard, R.R.L., Lorenzen, C.J., 1972. Yellow-green algae with chlorophyllide C1,2. J. Phycol. doi:10.1111/j.0022-3646.1972.00010.x.

Hoellein, T., Rojas, M., Pink, A., Gasior, J., Kelly, J., 2014. Anthropogenic litter in urban freshwater ecosystems: distribution and microbial interactions. PLoS One 9. doi:10.1371/journal.pone.0098485.

Jansson, C., Northen, T., 2010. Calcifying cyanobacteria-the potential of biomineralization for carbon capture and storage. Curr. Opin. Biotechnol. 21, 365–371. doi:10.1016/j.copbio.2010.03.017.

Kaiser, D., Kowalski, N., Waniek, J.J., 2017. Effects of biofouling on the sinking behavior of microplastics. Environ. Res. Lett. 12. doi:10.1088/1748-9326/aa8e8b.

Kamjunke, N., Böing, W., Voigt, H., 1997. Bacterial and primary production under hypertrophic conditions. Aquat. Microb. Ecol. 13, 29–35. doi:10.3354/ame013029.

Karakolis, E.G., Nguyen, B., You, J.B., Rochman, C.M., Sinton, D., 2019. Fluorescent dyes for visualizing microplastic particles and fibers in laboratory-based studies. Environ. Sci. Technol. Lett. 6, 334–340. doi:10.1021/acs.estlett.9b00241.

Kasprzak, P., Benndorf, J., Gonsiorczyk, T., Koschel, R., Krienitz, L., Mehner, T., Hülsmann, S., Schultz, H., Wagner, A., 2007. Reduction of nutrient loading and biomanipulation as tools in water quality management: long-term observations on Bautzen Reservoir and Feldberger Haussee (Germany). Lake Reserv. Manag. 23, 410–427. doi:10.1080/07438140709354027.

Kerimoglu, O., Rinke, K., 2013. Stratification dynamics in a shallow reservoir under different hydro-meteorological scenarios and operational strategies. Water Resour. Res. 49, 7518–7527. doi:10.1002/2013WR013520.

Kettner, M.T., Rojas-Jimenez, K., Oberbeckmann, S., Labrenz, M., Grossart, H.P., 2017. Microplastics alter composition of fungal communities in aquatic ecosystems. Environ. Microbiol. 19, 4447–4459. doi:10.1111/1462-2920.13891.

Koschel, R., Benndorf, J., Proft, G., Recknagel, R., 1983. Calcite precipitation as a natural control mechanism of eutrophication. Arch. Hydrobiol. 98, 380–408. doi:10.1007/springerreference_205967.

Kurmayer, R., Christiansen, G., Holzinger, A., Rott, E., 2018. Single colony genetic analysis of epilithic stream algae of the genus *Chamaesiphon* spp. Hydrobiologia 811, 61–75. doi:10.1007/s10750-017-3295-z.

Lagarde, F., Olivier, O., Zanella, M., Daniel, P., Hiard, S., Caruso, A., 2016. Microplastic interactions with freshwater microalgae: hetero-aggregation and changes in plastic density appear strongly dependent on polymer type. Environ. Pollut. 215, 331–339. doi:10.1016/j.envpol.2016.05.006.

Leiser, R., Wu, G.-M., Neu, T.R., Wendt-Potthoff, K., 2020. Biofouling, metal sorption and aggregation are related to sinking of microplastics in a stratified reservoir. Water Res., 115748 doi:10.1016/J.WATRES.2020.115748.

Li, M., Zhu, W., Guo, L., Hu, J., Chen, H., Xiao, M., 2016. To increase size or decrease density? Different *Microcystis* species has different choice to form blooms. Sci. Rep. 6, 1–10. doi:10.1038/srep37056.

Long, M., Moriceau, B., Gallinari, M., Lambert, C., Huvet, A., Raffray, J., Soudant, P., 2015. Interactions between microplastics and phytoplankton aggregates: impact on their respective fates. Mar. Chem. 175, 39–46. doi:10.1016/j.marchem.2015.04.003.

López-García, P., Kazmierczak, J., Benzerara, K., Kempe, S., Guyot, F., Moreira, D., 2005. Bacterial diversity and carbonate precipitation in the giant microbialites from the highly alkaline Lake Van, Turkey.. Extremophiles 9, 263–274. doi:10.1007/s00792-005-0457-0.

Macintyre, I.G., Prufert-Bebout, L., Reid, R.P., 2000. The role of endolithic cyanobacteria in the formation of lithified laminae in Bahamian stromatolites. Sedimentology 47, 915–921. doi:10.1046/j.1365-3091.2000.00327.x.

Martinez, R.E., Gardés, E., Pokrovsky, O.S., Schott, J., Oelkers, E.H., 2010. Do photosynthetic bacteria have a protective mechanism against carbonate precipitation at their surfaces? Geochim. Cosmochim. Acta 74, 1329–1337. doi:10.1016/j.gca.2009.11.025.

Ortíz-Caballero, Z.K., Rentería-Villalobos, M., Montero-Cabrera, M.E., Manjón-Collado, G., Santellano-Estrada, E., Rentería-Monterrubio, A., 2019. Fractionation of chemical species in surface water from El Granero reservoir, Chihuahua, Mexico.. Environ. Earth Sci. 78, 1–13. doi:10.1007/s12665-019-8756-4.

Parada, A.E., Needham, D.M., Fuhrman, J.A., 2016. Every base matters: Assessing small subunit rRNA primers for marine microbiomes with mock communities, time series and global field samples. Environ. Microbiol. 18, 1403–1414. doi:10.1111/1462-2920.13023.

Peraza Zurita, Y., Cultrone, G., Sánchez Castillo, P., Sebastián, E., Bolívar, F.C., 2005. Microalgae associated with deteriorated stonework of the fountain of Bibataúín in Granada, Spain. Int. Biodeterior. Biodegrad 55, 55–61. doi:10.1016/j.ibiod.2004.05.006.

R Core Team, 2018. R: A language and environment for statistical computing.

Rogers, K.L., Carreres-Calabuig, J.A., Gorokhova, E., Posth, N.R., 2020. Micro-by-micro interactions: how microorganisms influence the fate of marine microplastics. Limnol. Oceanogr. Lett. 5, 18–36. doi:10.1002/lol2.10136.

Rosenhahn, A., Schilp, S., Kreuzer, H.J., Grunze, M., 2010. The role of "inter" surface chemistry in marine biofouling prevention. Phys. Chem. Chem. Phys. 12, 4275–4286. doi:10.1039/c004746p.

Rueden, C.T., Schindelin, J., Hiner, M.C., DeZonia, B.E., Walter, A.E., Arena, E.T., Eliceiri, K.W., 2017. ImageJ2: ImageJ for the next generation of scientific image data. BMC Bioinformatics 18, 1–26. doi:10.1186/s12859-017-1934-z.

Schwarzenberger, A., Sadler, T., Von Elert, E., 2013. Effect of nutrient limitation of cyanobacteria on protease inhibitor production and fitness of *Daphnia magna*. J. Exp. Biol. 216, 3649–3655. doi:10.1242/jeb.088849.

Stabel, H.-H., 1988. Algal control of elemental sedimentary fluxes in Lake Constance. In: SIL Proceedings, 23, pp. 700–706. doi:10.1080/03680770.1987.11899696 1922-2010.

Staudt, C., Horn, H., Hempel, D.C., Neu, T.R., 2004. Volumetric measurements of bacterial cells and extracellular polymeric substance glycoconjugates in biofilms. Biotechnol. Bioeng. 88, 585–592. doi:10.1002/bit.20241.

Teranes, J.L., McKenzie, J.A., Bernasconi, S.M., Lotter, A.F., Sturm, M., 1999. A study of oxygen isotopic fractionation during bio-induced calcite precipitation in eutrophic Baldeggersee, Switzerland.. Geochim. Cosmochim. Acta 63, 1981–1989. doi:10.1016/S0016-7037(99)00049-6.

Tianzhi, W., Yunkai, L., Mingchao, L., Peiling, Y., Zhihui, B., 2014. Biofilms on the surface of gravels and aquatic plants in rivers and lakes with reusing reclaimed water. Environ. Earth Sci. 72, 743–755. doi:10.1007/s12665-013-2998-3.

Wang, S., Xue, N., Li, W., Zhang, D., Pan, X., Luo, Y., 2020. Selectively enrichment of antibiotics and ARGs by microplastics in river, estuary and marine waters. Sci. Total Environ. 708, 134594. doi:10.1016/j.scitotenv.2019.134594.

Wang, Y.W., Zhao, J., Li, J.H., Li, S.S., Zhang, L.H., Wu, M., 2011. Effects of calcium levels on colonial aggregation and buoyancy of Microcystis aeruginosa. Curr. Microbiol. 62, 679–683. doi:10.1007/s00284-010-9762-7.

Wu, X., Pan, J., Li, M., Li, Y., Bartlam, M., Wang, Y., 2019. Selective enrichment of bacterial pathogens by microplastic biofilm. Water Res. 165, 114979. doi:10.1016/j.watres.2019.114979.

Xu, H., Lv, H., Liu, X., Wang, P., Jiang, H., 2016a. Electrolyte cations binding with extracellular polymeric substances enhanced *Microcystis* aggregation: implication for *Microcystis* bloom formation in eutrophic freshwater lakes. Environ. Sci. Technol. 50, 9034–9043. doi:10.1021/acs.est.6b00129.

Xu, H., Yang, C., Jiang, H., 2016b. Aggregation kinetics of inorganic colloids in eutrophic shallow lakes: influence of cyanobacterial extracellular polymeric substances and electrolyte cations. Water Res. 106, 344–351. doi:10.1016/j.watres.2016.10.023.

Záray, G., Kröpfl, K., Szabó, K., Taba, G., Ács, É., Berlinger, B., Dogan, M., Salih, B., Akbulut, A., 2005. Comparison of freshwater biofilms grown on polycarbonate substrata in Lake Velence (Hungary) and Lake Mogan (Turkey). Microchem. J. 79, 145–148. doi:10.1016/j.microc.2004.08.012.

Zippel, B., Neu, T.R., 2011. Characterization of glycoconjugates of extracellular polymeric substances in tufa-associated biofilms by using fluorescence lectin-binding analysis. Appl. Environ. Microbiol. 77, 505–516. doi:10.1128/AEM.01660-10.